THE SYSTEM AM HER = 4U 1814 + 50

LUCIO CHIAPPETTI*, ENRICO G. TANZI, and ALDO TREVES

Istituto di Fisica dell'Università
and
Laboratorio di Fisica Cosmica del CNR, Milano, Italy

(Received 29 April, 1980)

Abstract. The binary system AM Herculis = 4U 1814 + 50 gives the first well ascertained example of an X-ray emitting magnetic white dwarf. The orbital period (3.1^h) is apparent from X-ray to IR frequencies and in linear and circular polarization. Since the time of the identification of the X-ray source the system has been extensively studied. The observations (which range from 1 MeV to 20 μm) are reviewed and compared with the present theory of X-ray emitting white dwarfs.

Contents

1. Introduction

The variable star AM Herculis was discovered by Wolf in 1924; the classification ranges from 'very irregular' (Beyer, 1950) and 'in part semiregular' (Meinunger, 1960) to 'RW Aurigae type' (Kukarkin *et al.*, 1969), 'similar to many U Gem variables' (Bond and Tifft, 1974) and 'cataclysmic variable of the U Gem or Z Cam type' (Berg and Duthie, 1977).

Interest was raised about AM Her by its identification with a high galactic latitude X-ray source, first proposed by Berg and Duthie (1977). The star was just outside the

* Present address: Mullard Space Science Laboratory, Holmbury St. Mary, Surrey, U.K.

Space Science Reviews **27** (1980) 3–33. 0038–6308/80/0271–0003 $04.65.

TABLE I

List of observations of AM Her

Date	Observatory	Notes	Source
70 Dec 71 Jun	Uhuru satellite	2–6 keV	Giacconi *et al.* (1974)
* 71 Dec 73 Apr	Uhuru satellite	2–6 keV	Murray and Ulmer (1976)
* 74 Apr	Steward	visible spectroscopy	Bond and Tifft (1974)
75 Feb Apr	Westerbork	radio (610 MHz)	Harris *et al.* (1977)
75 May	SAS-3 satellite	0.15–0.8 keV	Hearn *et al.* (1976)
75 May Oct	KPNO	visible photometry	Berg and Duthie (1977)
75 Oct	OSO-8 satellite	2–60 keV	Swank *et al.* (1977)
75 Oct	OSO-8 satellite	0.15–0.28 keV	Bunner (1978)
* 76 May	SAS-3 satellite	0.15–0.8 keV	Hearn *et al.* (1976, 1977)
* 76 May Nov	Mt. Wilson–Palomar	visible photometry	Priedhorsky and Krzeminski (1978)
76 Jun Aug	Arizona	visible photometry and polarimetry	Tapia (1977)
76 Aug Oct	KPNO–MRO	visible photometry	Szkody and Brownlee (1977)
76 Aug	Palomar	radial velocity measurement	Priedhorsky (1977)
76 Aug	KPNO	radial velocity measurement	Cowley and Crampton (1977)
76 Sep	RGO	high speed photometry	Bailey *et al.* (1977)
76 Sep	DAO	visible spectroscopy	Crampton and Cowley (1977)
76 Sep	Copernicus satellite	2–6 keV	private communication
76 Sep Nov	Prairie	visible photometry	Olson (1977)
76 Sep	Battelle	polarimetry	Michalsky *et al.* (1977)
76 Sep	Arizona	spectroscopy and polarimetry	Stockman *et al.* (1977)
76 Nov 77 Jan	MRO	visible photometry	Szkody (1978)
* 77 Feb	Ariel-5 satellite	40–800 keV	Coe *et al.* (1978)
* 77 Feb	Ariel-5 satellite	2–20 keV	unpublished
* 77 Feb Mar	MRO	visible photometry	Szkody (1978)
77 Apr	Hale	radial velocity measurement	Greenstein *et al.* (1977)
77 Apr	SAO	visible spectroscopy	Vojkhanskaja (1978)
77 Apr Sep	RGO	visible photometry and polarimetry	Bailey *et al.* (1978)
77 Jun Jul	Mt. Wilson–Palomar	visible photometry and polarimetry	Prieshorsky *et al.* (1978a)
77 Jun	Mt. Wilson	IR photometry	Priedhorsky *et al.* (1978b)
77 Jul	Steward	high speed polarimetry	Stockman and Sargent (1979)
77 Jul	Tenerife	IR photometry	Jameson *et al.* (1978)
77 Sep	MPI–AIT balloon	16–120 keV	Staubert *et al.* (1978)
77 Sep	Rocket	0.1–0.5 keV	Hayakawa *et al.* (1979)
77 Sep Oct	HEAO-I satellite	0.15–0.5 keV	Tuohy *et al.* (1978)
77 Sep Oct	HEAO-I satellite	2–60 keV	Swank (see Tuohy *et al.*, 1978)
77 Oct	OSO-8 satellite	2–250 keV	Coe *et al.* (1979)
77 Nov	LAS–Bologna	visible photometry	Gilmozzi *et al.* (1978)
78 Apr Jul	IUE satellite	UV spectroscopy	Tanzi *et al.* (1980)
78 May Jul	IUE satellite	UV spectroscopy	Raymond *et al.* (1979)
78 May Jul	Mt. Wilson–Palomar	IR spectroscopy	Young and Schneider (1979)
79 March	IUE satellite	UV spectroscopy	Raymond *et al.* (1979b)
79 March	Einstein satellite	1–3 keV	Fabbiano *et al.* (1980)
79 May	Hakucho satellite	0.1–0.3 keV	Nagase (1979)

Asterisks indicate observations in LO state.

Uhuru error box, but inside the error boxes of Ariel 5 and SAS 3 (Hearn *et al.*, 1976). The coordinates of the star AM Her are $\alpha_{1950} = 18^h14^m58^s.6$, $\delta_{1950} = 49°50'55''$ (Wright, 1977).

The identification was confirmed by the discovery of a common 3.1 hr periodicity in the X-ray (Hearn and Richardson, 1977) and visual light curves (Szkody and Brownlee, 1977), in the radial velocity (Cowley and Crampton, 1977; Priedhorsky, 1977) and in linear and circular polarization (Tapia, 1977).

The high ($\sim 10\%$) percentage of polarization allowed a first estimate of the magnetic field ($B \sim 10^8$ G): this fact and the similarity with cataclysmic variables led to the first models of the source. AM Herculis appears thus to be a binary system, containing a magnetic white dwarf and a non collapsed star. Accretion of matter onto the degenerate component would be the mechanism of X-ray emission.

Since the time of the identification with 4U 1813 + 50, many observations were made: they are listed in Table I and range from hard X-ray to IR (20 μm), including photometry, polarimetry and spectroscopy. An upper limit to radio emission from AM Her (< 55 mJy at 610 MHz) was obtained by Harris *et al.* (1977).

Detailed models have been proposed, with particular attention to the role of the magnetic field for the guidance of accretion and the origin of the UV, visible and IR spectra. The X-ray and UV spectra of AM Her proved also to be a very good test for the theories of X-ray emission by accreting magnetic white dwarfs.

In Section 2 the observations in the IR, visible and UV bands are reviewed. After a description of the 3.1 hr period modulated phenomena, the appearance of the spectrum (both line and continuum) and the variability of the source are discussed. The X-ray band observations are reviewed in Section 3. In Section 4, the models of AM Her are presented. Other sources of the same type of AM Her are briefly described in Section 5.

2. Optical Observations

2.1. Binary Period Modulation

Modulation with the binary period of 3.1 hr is observed in radial velocity, polarization and X-ray flux as well as photometrically. Here we concentrate on ultraviolet, U, B, V, and infrared light curves (see Figure 1).

Two phase conventions are in use: (1) the magnetic or polarization phase ϕ_m which refers to the maximum linear polarization (see Section 2.4); (2) the photometric phase ϕ_{ph} which refers to the V primary minimum. The epochs are (e.g. Crampton and Cowley, 1977):

$$\phi_m = 0 \quad \text{at} \quad \text{JD } 2\,443\,014.765\,,$$

$$\phi_{ph} = 0 \quad \text{at} \quad \text{JD } 2\,443\,014.713\,,$$

$$\phi_m = \phi_{ph} + 0.6\,.$$

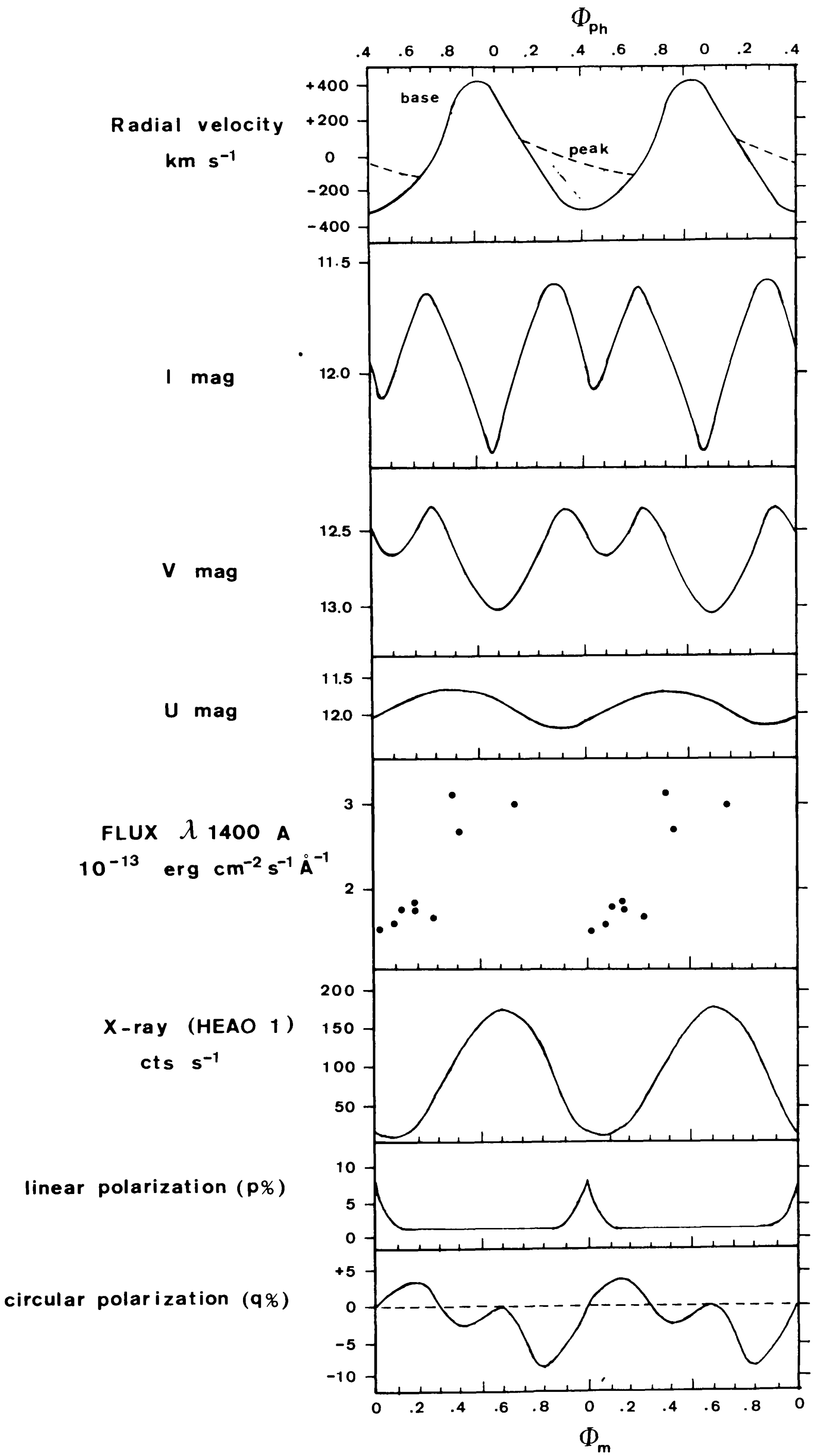

Fig. 1. Binary period ($P = 3.1^h$) modulation in AM Her. Radial velocity, U, V, I, X-ray and linear polarization q, are from Priedhorsky *et al.* (1978b, and references therein). Circular polarization p is from Tapia (1977) and the UV is from Raymond *et al.* (1979). (Adapted from Crampton and Cowley, 1977).

TABLE II

The period of AM Her

Period (JD)+		Method	Source
0.128 927	(2)	photometry	Szkody and Brownlee (1977)
0.128 918	(9)	polarimetry	Tapia (1977)
0.128 937	(5)	spectroscopy	Priedhorsky (1977)
0.128 922	–	average value	Priedhorsky (1977)
0.128 926	(9)	spectroscopy	Crampton and Cowley (1977)
0.128 924	(3)	photometry	Olson (1977)
0.128 928	(1)	photometry	Priedhorsky and Kzreminski (1978)
0.128 926 9	(7)	photometry	Priedhorsky *et al.* (1978a)
0.128 927 7	(7)	polarimetry	Priedhorsky *et al.* (1978b)
0.128 928	(1)	polarimetry	Stockman and Sargent (1979)
0.128 927 74	(12)	photometry and spectroscopy	Young and Schneider (1979)

The number in parentheses is the error on the last figure.

Because of its shortness, the value of the period is critical for a good phasing of observations: the available data are reported in Table II. No secular variation is apparent: $|\dot{p}/p| < 5 \times 10^{-14}\ s^{-1}$ (Young and Schneider, 1979).

The V light curve of AM Her shows a broad ($\Delta\phi \sim 0.6$), deep ($\Delta m \sim 0.7$) primary minimum and a shallower secondary minimum (Szkody and Brownlee, 1977; Olson, 1977; Priedhorsky and Krzeminski, 1978; Szkody, 1978; Gilmozzi *et al.*, 1978; Priedhorsky *et al.*, 1978a, b) which is not a permanent feature (Priedhorsky and Krzeminski, 1978; Szkody, 1978). Large flickering is apparent ($\Delta m \leqslant 0.2$ mag with time scales of hundreds of seconds (e.g., Szkody, 1978; Berg and Duthie, 1977)). Isolated flares appear sporadically (Priedhorsky and Krzeminski, 1978; Bailey *et al.*, 1978). A spike at the time of primary minimum was observed twice by Szkody and Brownlee (1977).

The relative importance of the two minima depends on the wavelength. In the most recent observations in the R($\lambda_{eff} \sim 0.7$ μm) and I($\lambda_{eff} \sim 0.9$ μm) bands, both minima are rather deep: their depths are $\Delta m \sim 1$ (primary) and $\Delta m \sim 0.5$ (secondary) (Gilmozzi *et al.*, 1978; Priedhorsky *et al.*, 1978a). In the J($\lambda_{eff} \sim 1.2$ μm) and H($\lambda_{eff} \sim 1.6$ μm) bands the depths become similar and in the K band ($\lambda_{eff} \sim 2.2$ μm) the secondary minimum is the prominent feature ($\Delta m \sim 0.2$), while the primary is smeared off ($\Delta m < 0.1$) (Priedhorsky *et al.*, 1978b; Jameson *et al.*, 1978).

At shorter wavelengths (U and B bands) the light curves are characterized by the absence of the secondary minimum. The primary minimum is offset in phase by 0.2 in the B band and by 0.3 in the U band (Szkody and Brownlee, 1977; Crampton and Cowley, 1977). In coincidence with the disappearance of the V secondary minimum Szkody (1978) reports a shift of the U minimum from (photometric) phase 0.3 to phase 0. However it is not clear whether the shift is necessarily correlated with the disappearance of the V secondary minimum or is a random variation. Flickering in the U band, correlated with flickering in V and at λ 4686 has been observed (Szkody and Margon, 1980).

An analysis of the colour indices by Gilmozzi *et al.* (1978) is interpreted as indicating that the U flux is due to two sources, one with a minimum at phase 0.3, another with the minimum at the same phase (0.55) of the X-ray one. These sources do not coincide with the major source of the V flux (Priedhorsky and Krzeminski, 1978).

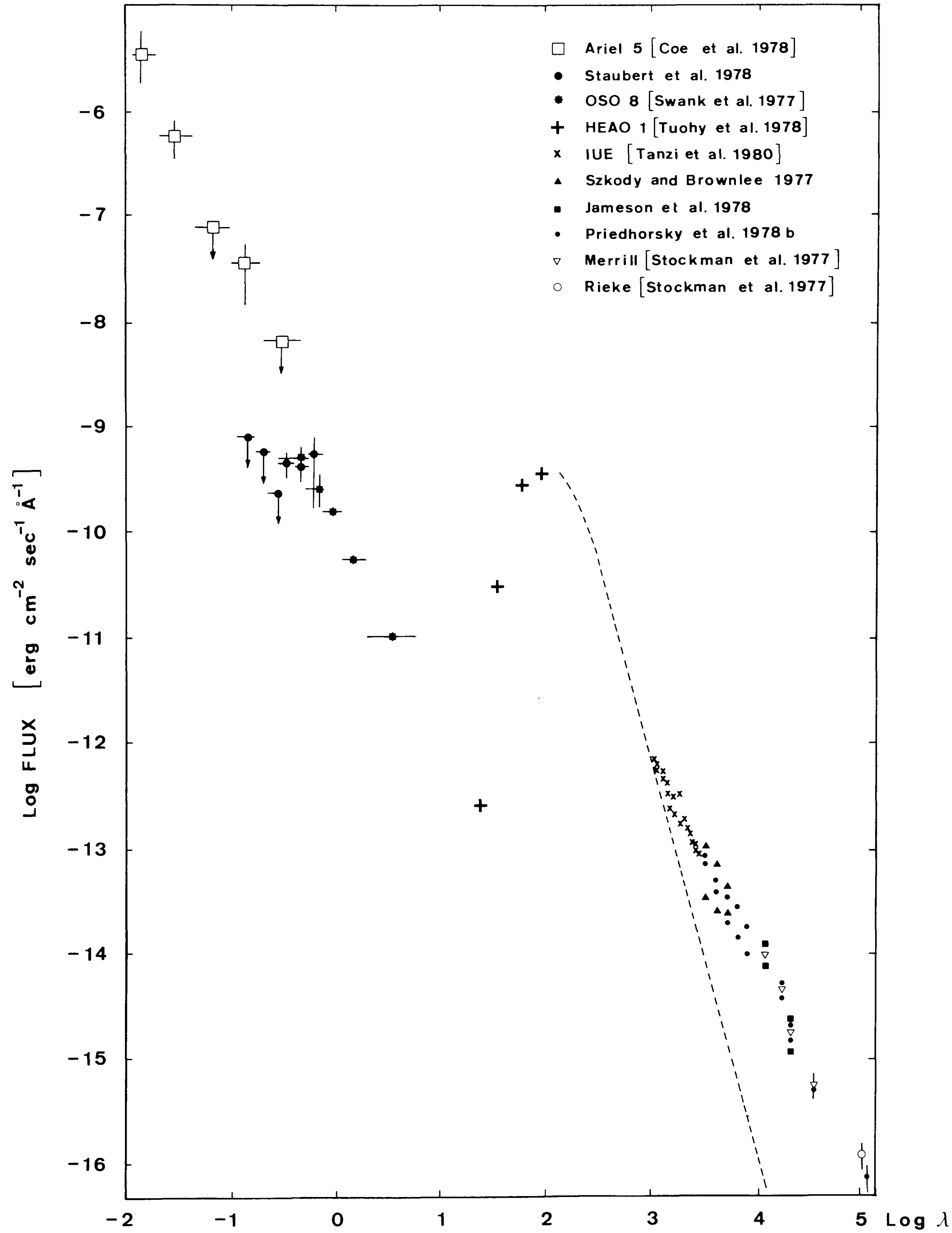

Fig. 2. Composite spectrum of AM Her. X-ray data are corrected for interstellar absorption with $N_H = 3.75 \times 10^{20}$ cm^{-2} and UV with $A_v = 0.08$. Dashed line is a blackbody with $kT = 25$ eV.

Variability in the ultraviolet (1000–3000 Å) was found by Raymond *et al.* (1979a). Shortwards of 2000 Å a single minimum is present, coincident in phase with the X-ray one. Its depth increases with wavelength. In the 2000–3000 Å region the flux is nearly constant with phase.

2.2. Spectrum: the continuum

Spectroscopic observations of AM Her have been made in the visible (Bond and Tifft, 1974; Crampton and Cowley, 1977; Stockman *et al.*, 1977), in the UV (Raymond *et al.*, 1979a, b; Tanzi *et al.*, 1979, 1980) and in the near IR (Young and Schneider, 1979). The system exhibits strong emission lines superimposed to a well defined continuum.

Informations on the energy distribution in the IR can also be inferred from available photometric data (Stockman *et al.*, 1977, Jameson *et al.*, 1978, Priedhorsky *et al.*, 1978b, Szkody and Capps, 1980).

A composite spectrum is shown in Figure 2. The UV points are dereddened with $A_v = 0.08$ (Tanzi *et al.*, 1979, 1980), which is consistent with the distance of AM Her (see Section 2.6) and the hydrogen column density inferred from X-ray observations (see Section 3). Outside the eclipse the UV (1100–3200 Å) data are well fitted by a power law $F_\lambda \sim \lambda^{-2}$ (Raymond *et al.*, 1979a; Tanzi *et al.*, 1979, 1980). At minimum light the spectrum is flatter ($\alpha = -1.16$) (Raymond *et al.*, 1979b).

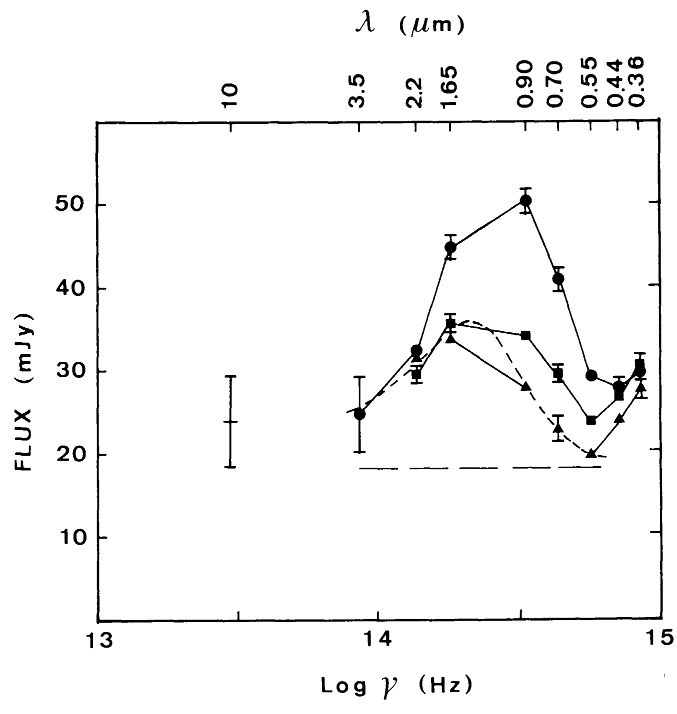

Fig. 3. Spectral energy distribution from 10 μm to 0.36 μm for the phases of maximum (●), primary minimum (▲), and secondary minimum (■). The 10 μm datum has insufficient time resolution to define a phase, while no 3.5 μm data are available for the phase of the minima. The heavy dashed line shows the sum of the energy distribution of an M2 V star plus that of a contribution which is flat with frequency (light dashed line). The solid lines are not a fit but are only an aid to the eye in coordinating the data with phase. (After Priedhorsky *et al.*, 1978b).

The λ^{-2} slope is on average acceptable also for the visible and IR data. A more careful examination of the energy distribution shows a slight shoulder at about 1 μm. The IR region of the spectrum is shown in Figure 3. Large variability on year time-scale in the IR bands is apparent. Evidence of an excess at 10 μm is reported by Szkody and Capps (1980), together with an indication of a turnover at 20 μm, where they obtain only an upper limit. At primary minimum, the energy distribution peaks at 1.64 μm; this is interpreted as due to the emission of an M2 V companion (Priedhorsky *et al.*, 1978b).

2.3. Spectrum: the lines

The spectrum of AM Her shows strong (permitted) emission lines. The most prominent are the Balmer lines, He II (λ 4686), He II (λ 1640) C IV (λ 1550), Si IV (λ 1400) and N V (λ 1240). The only absorption features are Na I ($\lambda\lambda$ 8138, 8194) (Young and Schneider, 1979) and, possibly, an unidentified feature at 7690 Å (Stockman *et al.*, 1977). A list of lines in the spectrum of AM Her is given in Table III; tracings are reported in Figure 4.

The radial velocity variation with the 3.1 hr period was discovered by Cowley and Crampton (1977) and Priedhorsky (1977). Since these early observations, an unusual phasing between the velocity and the light curves was apparent. In fact the maximum positive velocity coincides with the primary photometric minimum (see Figure 1), instead of being a quarter of period later, as expected for an ordinary spectrophotometric variable. This could be explained if the line emitting region is not located on the uncollapsed star.

From the absence of Zeeman splitting a lower limit to the distance of the line emitting region from the white dwarf surface can be deduced. This is 5 stellar radii for visible lines and 2.5 for UV lines (Stockman *et al.*, 1977; Greenstein *et al.*, 1977; Angel, 1978; Tanzi *et al.*, 1980). Therefore the lines are likely to be emitted by matter streaming between the two stars.

The Na I absorption lines are of stellar origin; from their presence and from limits on other absorption features Young and Schneider (1979) infer a spectral type M4–5V. The phasing of the light and absorption velocity curves is consistent with a stellar origin of the Na I lines.

The line variations are more complex than as due to simple radial velocity modulation. In the visible Cowley and Crampton (1977) consider three components of the line profiles (for the strongest lines): a broad base, a sharp peak and a weaker secondary component (not always present). Broad and sharp components have been detected also in the UV lines (Raymond *et al.*, 1979) and in the He I (λ 7065) (Young and Schneider, 1979). According to Crampton and Cowley (1977), the broad component yields a sinusoidal velocity curve (with amplitude of $\sim$ 400 km s^{-1}), while the sharp component is present only between (photometric) phases 0.2 and 0.8. Greenstein *et al.* (1977) examined the He λ 4471 and λ 4686 lines: the broad component is in good agreement with the results of Crampton and Cowley; a sinusoidal variation (amplitude $\sim$ 100 km s^{-1}) is found for the sharp component. The two

TABLE III

Lines in the spectrum of AM Her

Wavelength (Å)	Ion	W_λ (Å)	Source
1175–1176	C III	14	c, d
1206	Si III	10	c, d
1216	Lα	–	d
1239–1243	N V	18	c, d
1296–1300–1306	Si III–O I?	11	c, d
1334–1336–1338	C II–O IV?	11	c, d
1394–1403	Si IV	28	c, d
1548–1550	C IV	–	c, d
1640	He II	28	c, d
1885–1863	Al II–III	19	c, d
2306	He II	6	c
2733	He II	8	c
2796–2833	Mg II	22	c, d
3133	O III	17	a, c, d
3203	He II	–	a, c
3889	Hζ	–	a, b
3933	Ca II	3	b
3970	Hε + Ca II	–	a, b
4026	He I	7	a, b
4101	Hδ	–	a, b
4144	He I	2	b
4267	C II	2	a, b
4340	Hγ	~ 30	a, b
4471	He I	~ 10	a, b
4481	Mg II	–	b
4540	He II	2	a, b
4640–4650	C III–N III	7	a, b
4686	He II	~ 25	a, b
4713	He I	2	a, b
4861	Hβ	~ 30	a, b
4921	He I	5	a, b
5015	He I	–	a
5047	He I	–	a
5170	Fe II	–	a
5411	He II	–	a
5876	He I	–	a
6563	Hα	–	a
7065	He I	~ 4	e
7281	He I	~ 0.6	e
8498	Ca II	~ 0.7	e
8542	Ca II	~ 2	e
8662	Ca II	–	e
8193 (absorption)	Na I	~ 0.7	e
8194 (absorption)	Na I		e

Sources: a = Stockman *et al.* (1977).
b = Crampton and Cowley, 1977; they mention also Si II lines and Balmer lines up to H15.
c = Tanzi *et al.* (1980).
d = Raymond *et al.* (1979a).
e = Young and Schneider (1979).
Equivalent widths are taken from (c) in the UV and from (b) in the visible.

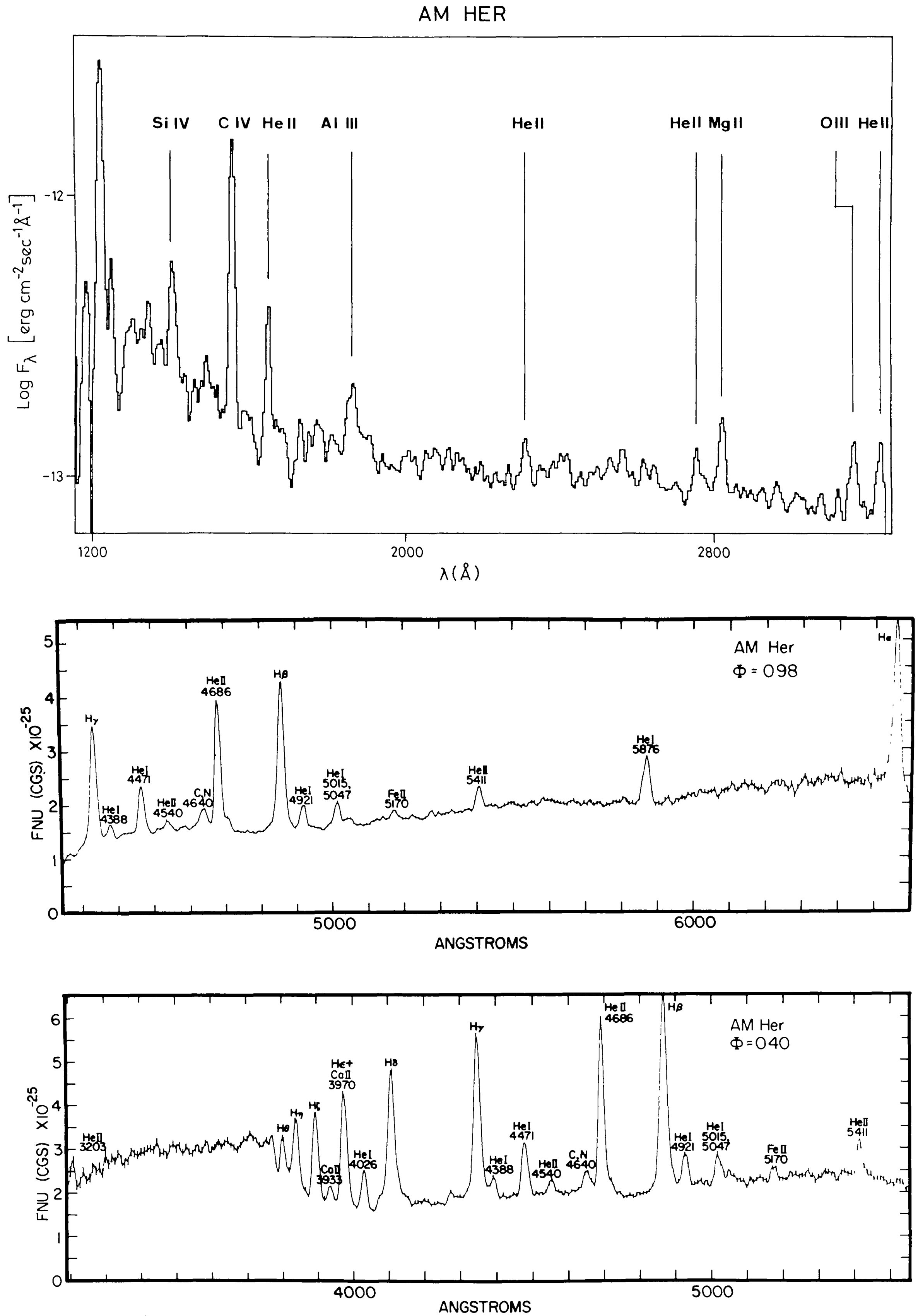

Fig. 4. Spectral tracings of AM Her. UV spectrum is from Tanzi *et al.* (1980). Visible spectra from Stockman *et al.* (1977).

components are out of phase by 133°. We note that in the phase interval 0.2–0.8 the sharp component of Crampton and Cowley and the sharp component of Greenstein *et al.* nearly coincide in phase.

A behaviour similar to that described by Greenstein *et al.* is reported by Young and Schneider (1979) for the He I (λ 7065) line. Also the absorption velocity curve (amplitude $\sim$ 170 km s^{-1}) displays a similar 135° phase difference (Young and Schneider, 1979) with respect to the broad component. Therefore the sharp emission component is likely to originate near the red dwarf, which is responsible of the absorption features.

Cowley and Crampton (1977) note that velocity curves of different ions are slightly out of phase, the maximum of the highest excitation lines occurring earlier. The amplitude of maxima decreases in the same way.

Variations of the equivalent widths of emission lines with phase are described by Crampton and Cowley (1977) in the visible, by Tanzi *et al.* (1979, 1980) in the UV and by Young and Schneider (1979) in the IR. The equivalent width is minimum about photometric phase 0 (primary minimum). The maximum occurs at phase 0.4 for the Balmer lines (at phase 0.5 if a correction for the continuum modulation is applied), between phases 0.4 and 0.6 for the He II (λ 4686) line, and at phase 0.2 for the UV lines (where, however, there is no complete phase coverage).

2.4. Polarization

Linear and circular polarization are modulated with the orbital period (Tapia, 1977). Linear polarization exhibits a sharp maximum ($p_{\max} = 6\%$) every period, while the circular polarization shows a more complex variation (see Figure 1) with $q_{\max} = -9\%$. According to further observations, the spike of linear polarization could be an intermittent feature (Tapia, private communication to Michalsky *et al.*, 1977): Bailey *et al.* (1978) observed a double peaked 2% maximum instead of Tapia's spike.

The correspondence of the linear polarization peak with a zero of circular polarization is indicative of a common origin of both polarizations. Polarization is observed in the V and I bands, while shortward of 4500 Å circular polarization is very little (Stockman *et al.*, 1977): an upper limit of 0.5% for linear polarization in the U band is reported by Tapia (1977).

Two mechanisms are usually invoked to explain polarization in white dwarfs: cyclotron radiation (e.g. Sazonov and Chernomordik, 1975; Ingham *et al.*, 1976) and magnetoemission (Kemp, 1970). In the former case one expects $p \sim q$, while in the latter $p \sim q^2$. In the case of AM Her on the basis of this criterion, cyclotron radiation is favoured by Chanmugan and Wagner (1977). The discovery of cyclotron absorption features in an object similar to AM Her is consistent with this interpretation (see Section 5). However the observations of Michalsky *et al.* (1977) are compatible with $p \sim q^2$.

The source of circular polarization is related to the source of visible and red (VR) flux. This is evinced from many indications: (a) VR photometric minima coincide with circular polarization standstills; (b) red flickering and flares tend to avoid these standstills; (c) the colour of the flares is similar to that of the light which is absent at the minima recall the colour dependence of polarization) (Priedhorsky and Krzeminski, 1978); (d) there is a significant correlation between flickering and circular polarization fluctuations (Bailey *et al.*, 1978; Priedhorsky *et al.*, 1978a; Stockman and Sargent, 1979).

The complex shape of the circular polarization curve derives from the fact that percentage polarization (and not the actual polarized flux) is measured; at certain phases polarized light can be more diluted.

2.5. Long term variations

AM Her exhibits active (HI) and inactive (LO) states both in visible and X-ray emission (for the latter see Section 3.2). From the examination of archive plates it was thought that these variations were periodic, with a period between 130 and 176 d (Meinunger, 1960, 1976; Hudec and Meinunger, 1976) or of 600–670 d (Liller, 1976). A full set of data between 1890 and 1976 has been examined by Feigelson *et al.* (1978) using a least-square technique; none of these periodicities appear to be real.

However AM Her exhibits transitions from ~ 12 to ~ 15 mag with an average duration of 100–300 days, being for most of the time in the HI state. This is opposite to the usual behaviour of cataclysmic variables, which are more often at minimum light with occasional outbursts. A light curve for 1976–1977 is given in Figure 5.

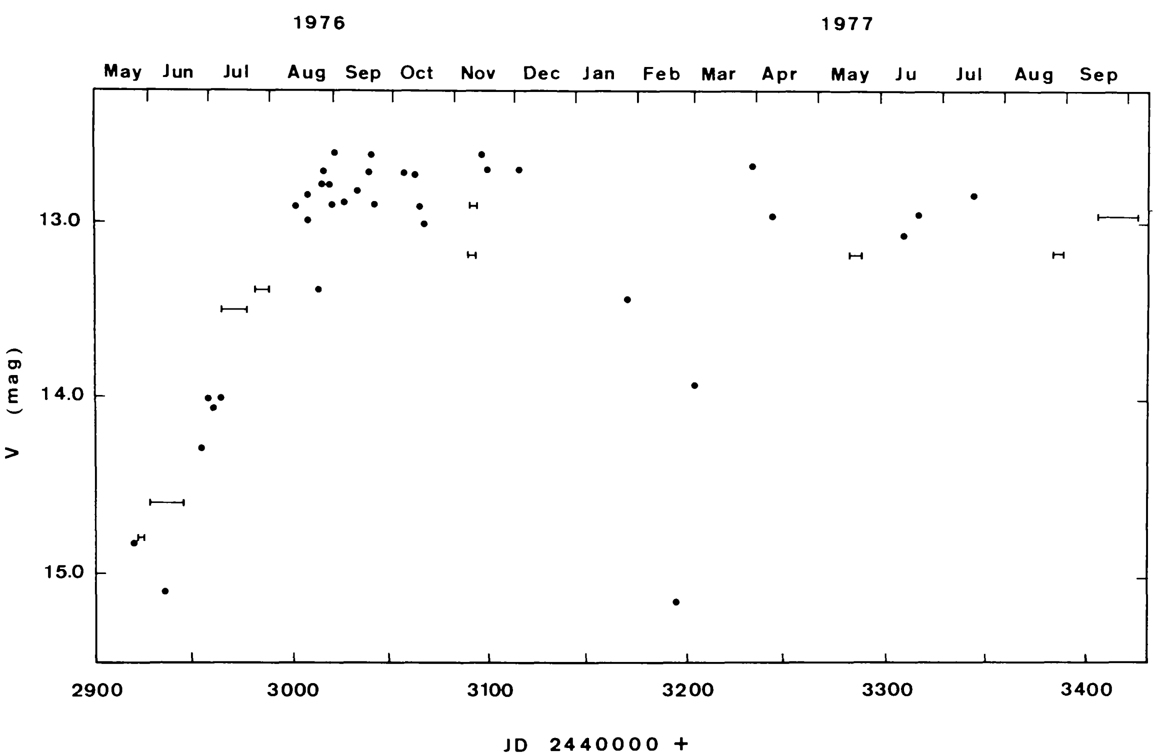

Fig. 5. V light curve for AM Her during 1976–77. The 1976 part is adapted from Crampton and Cowley (1977, see references therein). The 1977 data have been collected from the following sources: Bailey *et al.* (1977, 1978), Priedhorsky *et al.* (1978a, b), Szkody (1978).

Large irregular fast variability could have masked the binary modulation in the past, which explains the failure of Feigelson *et al.* (1978) to detect the binary period in their search.

Spectral variations are apparent by a comparison between the LO state data and HI state spectra (Bond and Tifft, 1974; Crampton and Cowley, 1977). In the LO state all lines are weaker and He II (λ 4686) is absent. In the HI state this line is one of the strongest features, comparable with the first Balmer lines (Crampton and Cowley, 1977; Stockman *et al.*, 1977; Vojkhanskaja, 1978).

2.6. System parameters

The main parameters of the system AM Her are listed in Table IV.

The existence in the system of a magnetic white dwarf is inferred from the high polarization (Tapia, 1977).

TABLE IV

Main parametres of AM Her

Distance	~ 100 pc
Period	3.1 hr
m_v (HI state)	11.9 mag
m_v (LO state)	15.0 mag
magnetic field	~ 10^8 G
semi-axis	0.7–0.9 10^{11} cm
mass of the white dwarf	$1M_\odot$
mass of the M2 V component	$0.4M_\odot$

Evidence of a red dwarf companion is given by IR observations of Priedhorsky *et al.* (1978b) (spectral type M2V) and of Young and Schneider (1979) (spectral type M4–5V), already quoted in Sections 2.2 and 2.3.

It is not possible to use the emission line mass function $f(m) = 0.4 \pm 0.1M_\odot$ for an estimate of the masses of the components, because, as noted, the radial velocities are not relative to the two stars. Assuming a secondary mass $0.22M_\odot$ for Young and Schneider's M4–5V star, the *absorption line* mass function $f(m) = 0.071 \pm 0.017M_\odot$ enables to deduce a mass ratio $q = 6.5$–1.25 and an inclination $i = 24°$–$70°$. If the line intensity minimum is a partial eclipse of the emitting region (Young and Schneider, 1979) then $i \simeq 40°$, and the primary mass $\sim 0.5M_\odot$. Priedhorsky *et al.* (1978b) quote a mass of $0.35M_\odot$ and a radius of 3×10^{10} cm for their M2V secondary. Similar results ($0.4M_\odot$) are obtained by Cowley and Crampton (1977) using an empirical mass-period relationship and by Stockman *et al.* (1977) from an upper limit to the brightness of the secondary. $0.4M_\odot$ is the minimum mass which assure Roche lobe filling (Cowley and Crampton, 1977). From these estimates it is also possible an evaluation of the semi-axis of the orbit: 0.7–1 $\times 10^{11}$ cm (Chanmugam and Wagner, 1977; Stockman *et al.*, 1977; Priedhorsky and Krzeminski, 1978).

The distance of AM Her may be estimated by (a) proper motion arguments (Stockman *et al.*, 1977, and references therein), (b) from the absolute magnitude (Chanmugam and Wagner, 1977; Priedhorsky *et al.*, 1978b; Young and Schneider, 1979), (c) from X-ray absorption (see Section 3). All these arguments yield a distance of ~ 100 pc.

The magnetic field intensity is evaluated from polarization. In the case of magneto-emission (see Section 2.4), the component of B parallel to the line of sight and the fractional circular polarization $q(\omega)$ at the frequency $2\pi\omega$ are related by (Kemp, 1970):

$$B_{\|} = m_e c\omega q(\omega)/e\,. \tag{2.1}$$

In the case of cyclotron emission the shortest wavelength with nonzero polarization is assumed the cyclotron frequency $\omega_c = eB/m_e c$ (Tapia, 1977). The order of magnitude of B is in both cases about 10^8 G.

3. X-Ray Observations

3.1. Binary period modulation

A modulation of the X-ray flux with the 3.1 hr binary period has been observed both in soft (Hearn and Richardson, 1977; Bunner, 1978; Tuohy *et al.*, 1978; Nagase, 1979) and hard X-rays ($\leqslant 60$ keV) (Swank *et al.*, 1977). Due to poor time resolution no conclusive results were obtained at higher energies (Coe *et al.*, 1978). The light curve exhibits a minimum at the same phase of the visible secondary minimum: according to Hearn and Richardson (1977), Swank *et al.* (1977) and Bunner (1978), it is due to an eclipse, while Tuohy *et al.* (1978) report a nonzero residual flux (5% of maximum flux). A feature common to all soft X-ray light curves is an ingress steeper than egress (see Figure 1). The temporary occurrence of a secondary X-ray minimum at $\phi_m = 0.47$ is reported by Tuohy *et al.* (1980). Also the X-ray primary minimum is not a permanent feature. Priedhorsky and Krzeminski (1978) report that its disappearance is concurrent with that of the visible secondary minimum and of the circular polarization standstill.

The origin of the modulation in X-rays and in the optical is discussed in Section 4.

3.2. HI and LO states

Evidence of a long term variability of the X-ray source was known before the identification with AM Her. In fact the flux reported by the 3U catalog is about 3 times that of later Uhuru observations (Murray and Ulmer, 1976). These variations are probably correlated with the HI–LO optical states (see Table V). A decrease of an order of magnitude in soft X-ray flux is observed during the LO state of May 1976 (Hearn and Richardson, 1977) with respect to the preceding and following HI states (Bunner, 1978; Tuohy *et al.*, 1978). During the recovery to the HI state of November 1976 (Hearn, private communication to Priedhorsky and Krzeminski, 1978) the flux increased only by a factor 2: at that time the X-ray minimum disappeared (Priedhorsky and Krzeminski, 1978).

TABLE V

Optical and soft X-ray observations of AM Her

Date	m_v	X-ray flux (10^{-11} erg cm^{-2} s^{-1})	X-ray band	X-ray minimum
1975 Oct	12.6[a]	39[b]	0.15–0.28[b]	present[b]
1976 May	14.8[c]	3.3[d]	0.1 –0.3[d]	present[d]
1976 Nov	13.2[e]	~ 7[f]	0.1 –0.3[f]	absent[f]
1977 Sep	13[g]	50[h]	0.15–0.3[h]	present[h]
1977 Sep	–	31[i]	0.1 –0.28[i]	–
		50[i]	0.1 –0.5[i]	–
1979 May	–	38[l]	0.1 –0.3[l]	present[l]

Adapted from Tuohy *et al.* (1978).

Sources: a = Berg and Duthie (1977).
b = Bunner (1978).
c = Berg (see Touhy *et al.*, 1978).
d = Hearn and Richardson (1977).
e = Priedhorsky and Kzreminski (1978).
f = Hearn (see Touhy *et al.*, 1978).
g = Tapia (see Touhy *et al.*, 1978).
h = Tuohy *et al.* (1978).
i = Hayakawa *et al.* (1979).
l = Nagase (1979).

During the LO state of February–April, 1977, Ariel 5 X-ray observations show an increase at higher energy (see next section) while at medium energy (2–10 keV) the source was not visible above the background (Sanford, private communication). No observations in the soft X-rays are reported.

The association of a decrease in soft X-rays and an increase in hard X-rays would not be surprising. An increase in the accretion rate would indeed increase the X-ray luminosity and the comptonization, cancelling the high energy tail.

3.3. X-RAY SPECTRUM

The X-ray spectrum is derived from observations by Swank *et al.* (1977), Coe *et al.* (1978, 1979), Bunner (1978), Tuohy *et al.* (1978), Staubert *et al.* (1978), Hayakawa *et al.* (1979), Nagase (1979), and Tuohy *et al.* (1980) (see Figures 6 and 2). Values of flux and luminosity (without correction for interstellar absorption) are collected in Table VI.

The X-ray spectrum of AM Her is generally interpreted as a two-component spectrum; parameters of various fits are shown in Table VII.

Hearn *et al.* (1976) proposed a single fit (power law with spectral index -2.5) combining SAS 3 (0.15–0.28 keV) and Uhuru (2–6 keV) measurements: however this result is obtained using observations taken at different epochs and in not contiguous bands.

The soft (< 0.5 keV) X-ray observations are fitted either by a Bremsstrahlung spectrum or by a blackbody one. Bunner (1978), Tuohy *et al.* (1978), Hayakawa *et al.*

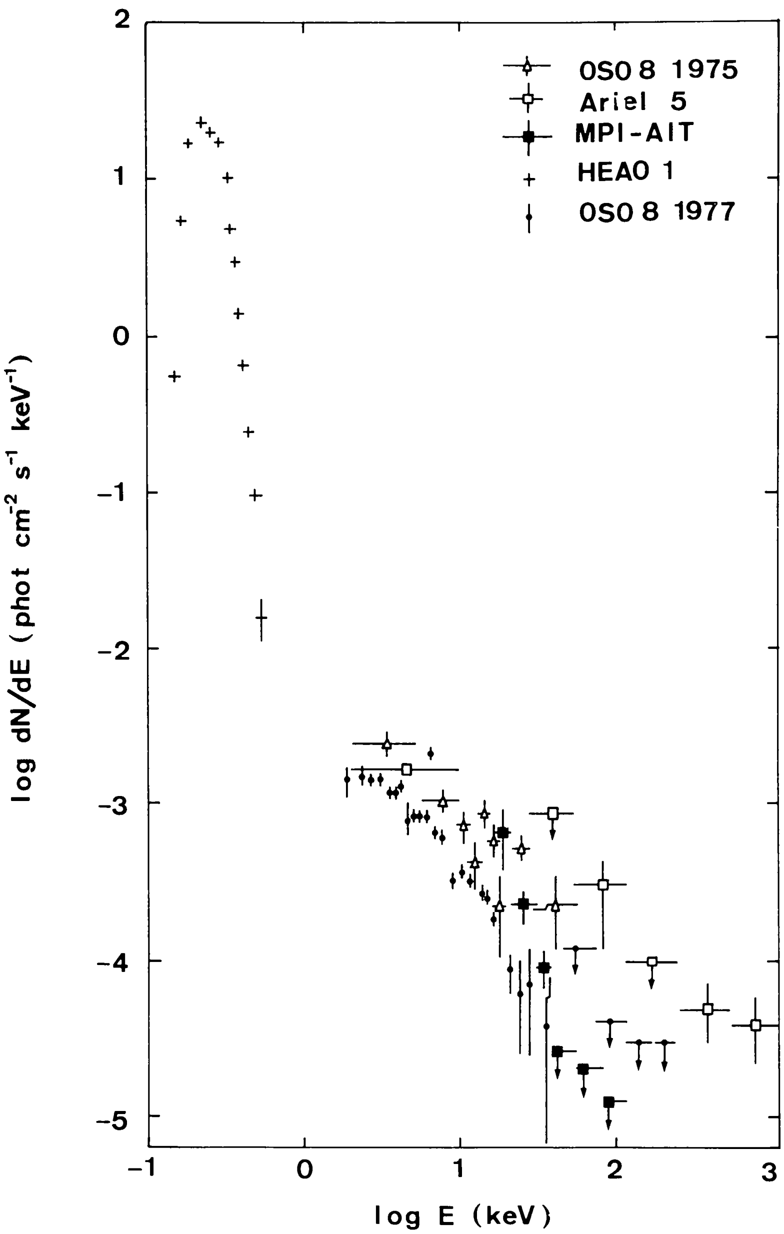

Fig. 6. X-ray photon spectrum of AM Her, corrected for interstellar absorbtion with $N_H = 3.75 \times 10^{20}$ cm^{-2} (Sources: HEAO-1: Tuohy *et al.* (1978); OSO-8: 1975, Swank *et al.* (1977); MPI-AIT: Staubert *et al.* (1978); ARIEL-5: Coe *et al.* (1978); OSO-8: 1977, Coe *et al.* (1979).

(1979), and Nagase (1980) consider both cases, obtaining a temperature of several 10^5 K (for details see Table VII). There are theoretical reasons (see Section 4) in favour of the blackbody fit.

A good fit of the OSO-8 1975 hard X-ray observations (Swank *et al.*, 1977; Bunner, 1978) is difficult: if the emission is thermal the temperature is very high (2×10^9 K) otherwise a power law with spectral index from -0.4 to -0.9 is acceptable. OSO-8 1975 data match well with both Ariel-5 measurements (Coe *et al.*, 1978) and the balloon observations of Staubert *et al.* (1978). At higher energies the latter measure-

TABLE VI

Flux and luminosity of AM Her in various spectral regions. No correction for interstellar absorbtion and reddening has been made

Band (keV)	Flux ($erg\ cm^{-2}\ s^{-1}$)	Luminosity ($10^{32}\ erg\ s^{-1}$)	Source
1–1000	–	5	Coe *et al.* (1978)
> 2	–	4	Staubert *et al.* (1978)
2–60	7.6×10^{-10}	9.1	Swank *et al.* (1977)
10–60	6.6×10^{-10}	–	Swank *et al.* (1977)
2–60	–	3	Swank (see Tuohy *et al.*, 1978)
2–18	1.05×10^{-10}	–	Cooke *et al.* (1978)
2–10	1.1×10^{-10}	–	Bunner (1978)
2–6	5.2×10^{-11}	–	Swank *et al.* (1977)
2–6	8.7×10^{-11}	–	Giacconi *et al.* (1974)
2–6	3×10^{-11}	–	Murray and Ulmer (1976)
0.1–3	–	1.1	Tuohy *et al.* (1978)
0.4–0.8	4.5×10^{-11}	–	Hearn *et al.* (1976)
0.15–0.28	6.5×10^{-11}	–	Hearn *et al.* (1976)
0.19–0.28	1.6×10^{-10}	2	Swank *et al.* (1977)
0.19–0.28	1.3×10^{-10}	–	Bunner (1978)
0.15–0.28	3.9×10^{-10}	8.5	Bunner (1978)
0.15–0.3	5×10^{-10}	–	Tuohy *et al.* (1978)
0.15–0.5	8×10^{-10} (a)	–	Tuohy *et al.* (1978)
0.1–0.28	3.1×10^{-10}	–	Hayakawa *et al.* (1979)
0.1–0.5	5.0×10^{-10}	–	Hayakawa *et al.* (1979)
0.1–0.5	1.2×10^{-10}	–	Tuohy *et al.* (1980)
0.1–0.5	7.6×10^{-10}	–	Tuohy *et al.* (1980)
0.1–0.3	3.8×10^{-10}	–	Nagase (1979)
UV (1000–3000 Å)	–	7	based on Tanzi *et al.* (1979)
Visible (3000–10 000 Å)	–	1.8	Swank *et al.* (1977)
IR (1–10 μm)	–	1.2	Swank *et al.* (1977)

(a) At light curve maximum.

ments are not in mutual agreement. Ariel-5 reveals a power law (-0.84) spectrum extending to about 800 keV while Staubert *et al.* observe a Bremsstrahlung spectrum ($T \sim 2 \times 10^8$ K) which drops at about an order of magnitude below that of Ariel-5 and matches better with the OSO-8 1975 data. We note that Ariel-5 observations were the only ones made in a LO state. The OSO-8 1977 data (Coe *et al.*, 1979; Pravdo, 1978) taken a few days after the balloon ones, may indicate a medium term variation in intensity and in spectral shape.

4. Models of the System

4.1. X-RAY EMITTING WHITE DWARFS

Before considering models of AM Her, we describe shortly the theory of accretion onto white dwarfs.

TABLE VII

Parameters of various fits for the X-ray spectrum of AM Her

Power law		Blackbody		Bremsstrahlung		Source
Spectral index	N_H†	T_{bb}	N_H†	T_{Br}	N_H†	
-2.5^a	$< 4.3^a$	–	–	–	–	Hearn *et al.* (1976)
-0.9^b	10^b	$3 \times 10^{5\,c}$	–	$4 \times 10^{5\,c}$	0.5^c	Bunner (1978)
-0.4^b	400^b	–	–	$2 \times 10^{9\,b}$	300^b	Swank *et al.* (1977)
-0.84^b	–	–	–	$5 \times 10^{9\,b}$	–	Coe *et al.* (1978)
–	–	–	–	$2 \times 10^{8\,b}$	–	Staubert *et al.* (1978)
–	–	$< 4.85 \times 10^5$	$> 1.7^c$	$< 5.8 \times 10^5$	$> 2.8^c$	Tuohy *et al.* (1978)
		$> 1.86 \times 10^5$	$< 6.5^c$			
–	–	$< 4 \times 10^5$	$> 0.7^c$	6×10^5	0.75^c	Hayakawa *et al.* (1979)
		$> 1.5 \times 10^5$	$< 2.5^c$			
–	–	$< 4 \times 10^5$	$> 0.5^c$			Nagase (1979)
		$> 2 \times 10^5$	$< 1.5^c$			
–	–	2.55×10^5	2.7^c	3.48×10^5	2.9^c	Tuohy *et al.* (1980)

† In 10^{20} cm^{-2}.
[a] Fit of the whole spectrum.
[b] Fit of the hard ($\geqslant$ 2 keV) X-ray part.
[c] Fit of the soft (0.1–0.5 keV) X-ray part.

The association between an X-ray source, namely Sco X-1, and an accreting white dwarf was first suggested by Cameron and Mock (1967). Hoshi (1973), Aizu (1973), and De Gregoria (1974) gave quantitative detailed pictures of the process of accretion onto white dwarfs. More recent works are those of Fabian *et al.* (1977), Katz (1977), Masters *et al.* (1977), Kylafis (1978), Masters (1978), Kylafis and Lamb (1979), and Lamb and Masters (1979).

We consider first the simpler case when the white dwarf has no magnetic field. We assume that accretion is spherical and accreted matter is fully ionized.

At a certain height above the surface a standing shock is formed. Matter is heated to the shock temperature

$$T_s = \tfrac{3}{8} T_{ff} = \frac{3}{8} \frac{GMm_p u}{kR} = 3.7 \times 10^8 \frac{M}{M_\odot} R_9^{-1} \tag{4.1}$$

and the distance of the shock to the white dwarf surface is

$$d = \frac{L}{4\pi R^2 \varepsilon} \tag{4.2}$$

(Fabian *et al.*, 1977), where M and R are respectively mass and radius of the white dwarf, ε is the cooling rate, L is the accretion luminosity

$$L = \frac{GM\dot{M}}{R} \tag{4.3}$$

and $\dot{M}$ the accretion rate. The dominant cooling mechanism is usually supposed to be Bremsstrahlung ($\varepsilon = \varepsilon_{ff}$); the balance among various cooling and heating processes is reviewed by Kylafis (1978).

Introducing in Equation (4.2) the explicit expression for ε_{ff}, it turns out that $d \sim \dot{M}^{-1}$; another important relation is between electron scattering optical depth (which is indicative of the importance of comptonization) and the accretion rate: $\tau_{es} \sim \dot{M}$.

The location of the shock, the luminosity and comptonization together with the radius R of the white dwarf determine the shape of the spectrum. Since R depends only on the mass, and the other quantities on $\dot{M}$, one can represent the various spectral regimes in a $M - \dot{M}$ plane (see Figure 7; Katz, 1977; Kylafis and Lamb, 1979).

Regime I is characterized by high accretion rates, $d \ll R$ (shock close to the surface), $\tau_{es} > 1$: the spectrum of the emitted radiation is degraded by Compton effect. In regime II (moderate accretion rate) $d \ll R$ but $\tau_{es} < 1$: radiation is effective in cooling

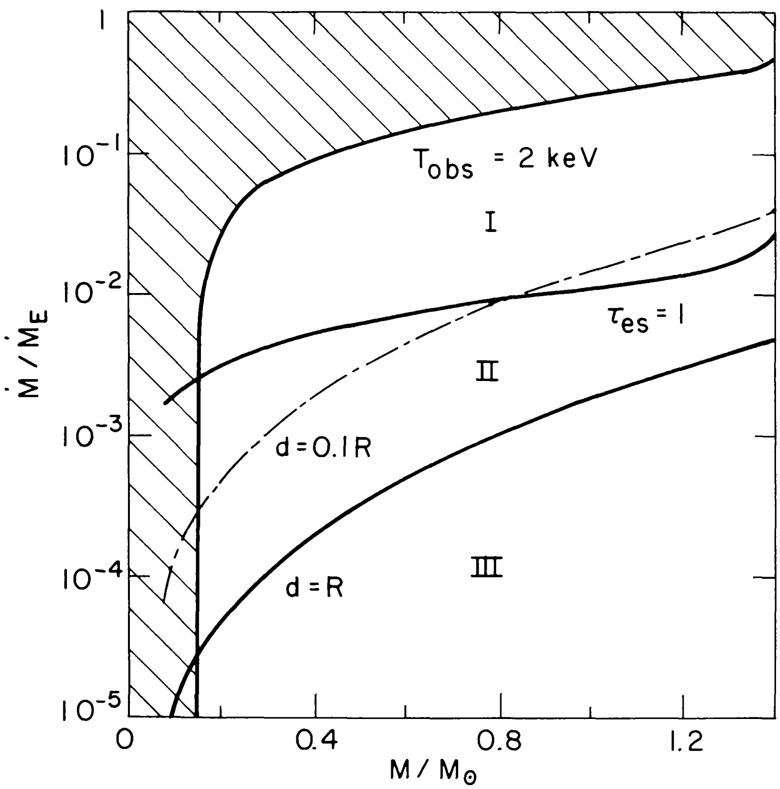

Fig. 7. Parameter regimes for accreting non magnetic white dwarfs in the ($\dot{M}/\dot{M}_E$, $M/M_\odot$)-plane. $\dot{M}_E$ is the Eddington accretion rate. Along the dashed curves the freefall time scale equals the Bremsstrahlung and Compton cooling times: $\tau_{ff}(R) = \tau_{br}(R)$ and $\tau_{ff}(R) = \tau_c(R)$. Below the solid curve labelled $d = R$, cooling of the hot, post-shock matter as it reaches the stellar surface requires a shock standoff distance $d > R$; above the curve $d < R$. Along the dot-dashed curve, $d = 0.1R$ as determined from detailed calculations. Above the solid curve labelled $\tau_{es} = 1$, the electron scattering optical depth from the stellar surface to infinity exceeds unity, and Compton scattering degrades the hard X-ray spectrum produced in the emission region. Above the solid curve labelled $T_{obs} = 2$ keV, a Bremsstrahlung fit to the observed X-ray spectrum gives a temperature less than 2 keV and the star ceases to be hard X-ray source (shaded region). The solid curves labelled $\tau_{es} = 1$ and $d = R$ divide accretion onto non magnetic degenerate dwarfs into three parameter regimes, labelled I, II, and III. (After Kylafis and Lamb, 1979).

matter, but the comptonization is negligible. According to Kylafis and Lamb (1979) this regime does not occur in practice. A low accretion rate and a shock far from the surface ($d \gg R$) are typical of regime III: $\tau_{es} < 1$, so that radiation aan freely escape.

In each regime the spectrum is formed by two components. Hard X-rays are emitted by Bremsstrahlung from the infalling matter in the hot post-shock region

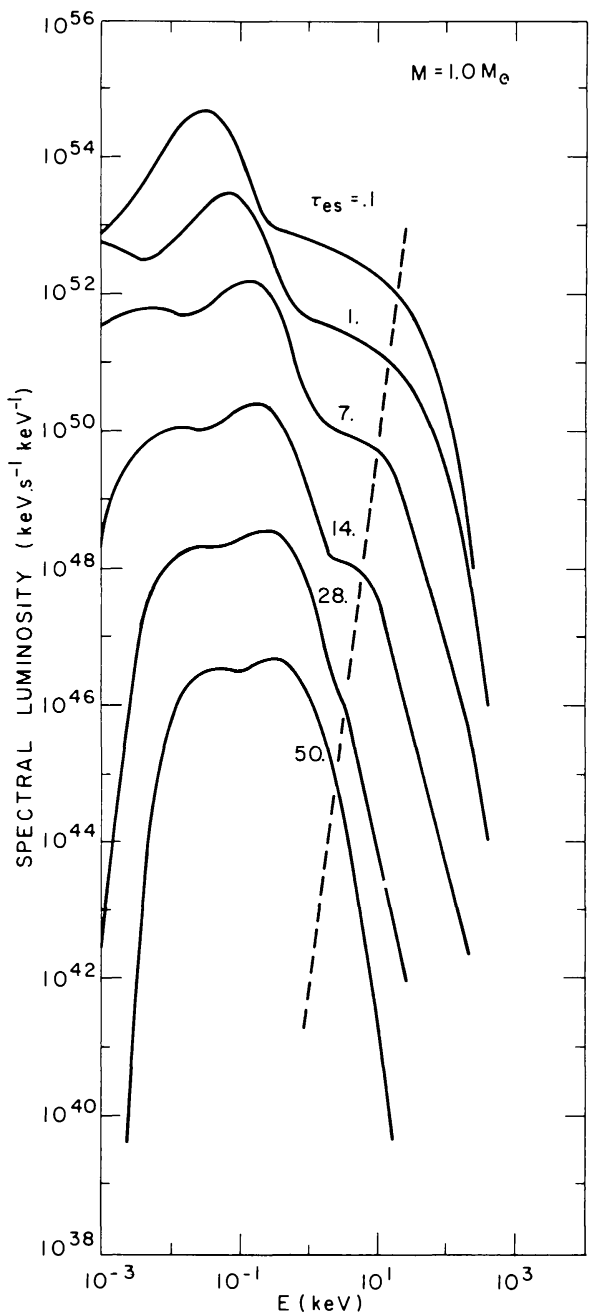

Fig. 8. Spectra produced by a $1.2M_{\odot}$ nonmagnetic dwarf for $\tau_{es} = 0.1$, 1, 7, 14, 28, and 50. The dashed lines indicate the increasing temperature of the blackbody peak and the decreasing energy of the hard X-ray cutoff, produced by Compton scattering, as the accretion rate increases. The units in ordinate correspond to the $\tau_{es} = 0.1$ curve; the other spectra have been multiplied by larger powers of 10. (After Kylafis and Lamb, 1979).

(the spectrum is more complex than an exponential + Gaunt one, because the post-shock region is not isothermal; Kylafis, 1978). Part of the Bremsstrahlung is intercepted by the surface of the white dwarf, thermalized and re-emitted as blackbody radiation in soft X-rays. In regime I the high energy component is partly degraded; Compton effect causes also a further heating of matter which emits 'secondary' radiation (a characteristic shoulder between the blackbody peak and the high energy tail). For very high accretion rates the hard X-ray component is completely cancelled out and only the blackbody one remains. The dependence of the spectral shape with $\dot{M}$ is shown in Figure 8.

With the same assumption, the effect of steady nuclear burning has been investigated by Weast *et al.* (1979) (see ref. therein for a discussion of the occurrence of either nuclear outbursts or steady burning). Burning occurs deep under the surface of the white dwarf. The energy emitted is transported to the surface and greatly enhances the blackbody component. Compton cooling is also enhanced so that hard X-ray luminosity is reduced and the spectrum is softened.

The presence of a magnetic field modifies this picture in two points: accretion is channelled by the field lines, and cyclotron emission becomes important. Since radiation can escape through the sides of the accretion column, the role of comptonization is also reduced. Accreting magnetic white dwarfs have been studied by Fabian *et al.* (1977), Masters *et al.* (1977), Lamb and Masters (1979), and King and Lasota (1979, 1980).

The Alfvén surface, i.e. the surface outside which the magnetic field has negligible interaction with infalling matter, is approximated by a sphere, whose radius R_A is obtained equating the energy density of the magnetic field and the kinetic energy density of matter (see e.g. Lamb *et al.*, 1973)

$$\frac{B^2(R_A)}{8\pi} = \frac{\rho(R_A)v^2(R_A)}{2}. \tag{4.4}$$

In the case of radial infall and for slow rotating white dwarfs the density ρ and the velocity v assume their free-fall values. For fast rotators, the magnetic energy density must be equated to the rotational energy density $\rho R_A^2\Omega^2/2$, and for matter in an accretion disk is equated to the Keplerian energy density $\rho GM/2R_A$.

Outside the Alfvén surface the flow of matter can be spherical, radial, etc., but within the Alfvén radius the infall is limited to a funnel, determined by the magnetic surface of equatorial radius R_A. Thus two accretion columns are formed above the magnetic poles: only a reduced fraction f of the white dwarf surface is hit by the accreting matter. For instance, for a surface dipole field of 10^8 G, and $R_A = 100R$ the half opening angle of the accretion column at the pole is 6°, that is $f = 3 \times 10^{-3}$.

A standing shock forms in the column; the spectrum is similar to that previously described, except that cyclotron cooling is active. Both Masters (1978) and King and Lasota (1979) distinguish two cases. When $\dot{M}$ is sufficiently large (with respect to the magnetic field), the electrons reach the shock temperature and Bremsstrahlung dominates. Otherwise cyclotron cooling can be so efficient, that electrons never reach the shock temperature (two fluid regime; more complicated regimes for increased values of B are described by Lamb and Masters (1979), see also Masters (1978).

The cyclotron emission occurs in the high harmonics (see e.g. Chanmugam and Wagner, 1979), since the first harmonics are self-absorbed. The spectrum has three components: the Bremsstrahlung and blackbody ones, as in the non-magnetic case; the third is the cyclotron component, dominant in the UV. At frequencies where cyclotron is self-absorbed, the spectrum has a Rayleigh-Jeans slope up to the frequency where radiation is freely emitted, and then falls abruptly (see Figure 9).

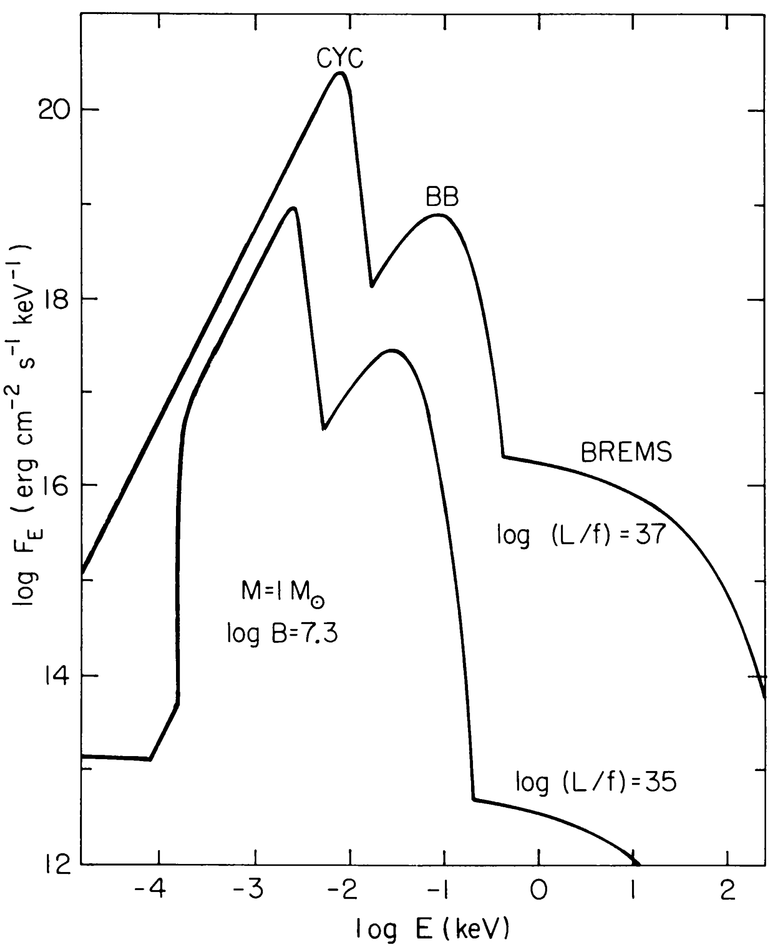

Fig. 9. X-ray and UV spectrum produced by two different accretion rates onto a $1M_{\odot}$ degenerate dwarf having a magnetic field of $B = 2 \times 10^7$ G. The portion of each spectrum below 5 eV is less certain due to possible additional flux from the heated stellar surface. (After Lamb and Masters, 1979).

4.2. Interpretation of the Spectrum of AM Her

The spectrum of AM Her, extending from IR to hard X-rays, is reported in Figure 2, where the UV and V fluxes have been corrected assuming a visual extinction $A_v = 0.08$ mag (Tanzi *et al.*, 1980) and the X-rays taking a hydrogen column density $N_H = 3.75 \times 10^{20}$ cm^{-2} (Tuohy *et al.*, 1978). Three components can be identified: (a) hard X-rays (3–60 keV); (b) soft X-rays (0.1–0.5 keV); (c) visible, UV, IR (10–0.1 eV).

Within the models described in the previous section one is led to interpret the hard X-rays as due to the Bremsstrahlung from the heated atmosphere and the soft X-ray peak as the black body emission of the radiation reprocessed by the white dwarf. In the UV Raymond *et al.* (1979a, b) find a dependence of the spectral shape with phase, which suggests the presence of a component with a $\lambda^{-3.75}$ slope, which is eclipsed, and a steady $\lambda^{-1.16}$ component, similar to that proposed also by Stockman *et al.* (1977) as an extrapolation of visible photometry. The sum of the two power laws yields an average spectrum $\sim \lambda^{-2}$ (see Tanzi *et al.*, 1980). The λ^{-4} power law is probably the tail of the blackbody observed in soft X-rays. However the self-absorbed cyclotron radiation (the spectral shape of which should be λ^{-4}) is not observed in contrast with the expectations of the model. This is consistent with the lack of polarization shortward of 4500 Å.

It is nevertheless possible that fundamental harmonic cyclotron emission is responsible of the polarized 'red' (V to I bands) flux. Flux at long wavelengths will be emitted at the cyclotron frequency in a lower magnetic field, i.e. at a greater distance from the white dwarf. If the primary minimum is due to obscuration of the emitting region by the body of the white dwarf (see next section), its width should decrease towards longer wavelengths (Priedhorsky and Krzeminski, 1978), which is consistent with the observations (Priedhorsky *et al.*, 1978b).

King and Lasota (1979) pointed out that another difficulty of the model derives from the luminosity balance among the components of the spectrum. A fraction

$$g(r) = \tfrac{1}{2} l - \left(l - \frac{R^2}{r^2} \right)^{1/2} \tag{4.5}$$

of the 'primary' (i.e. Bremsstrahlung plus cyclotron) radiation emitted at r will be intercepted by the stellar surface and contributes to the blackbody component (Kylafis, 1978). In a first approximation $g = \frac{1}{2}$. Therefore one expects

$$L_{bb} \sim L_{Br} + L_{cyc} \quad \text{and} \quad L_{bb} + L_{Br} + L_{cyc} = L = \frac{GM\dot{M}}{R}$$

L_{Br} (i.e. the hard X-ray luminosity) and L_{cyc} (or better the UV, V, IR luminosity 1000–100 000 Å) are known; the value of L is more uncertain because of interstellar absorption and of the relatively poor spectral resolution and narrow energy band of current soft X-ray instrumentations. The sum of the IR, V, and UV luminosities (see table VI) is $\sim 10^{33}$ erg s^{-1}: the hard X-ray luminosity is less than 9×10^{32} erg s^{-1} (we note incidentally that their sum is about equal to the soft X-ray observed luminosity reported by Tuohy *et al.* (1978)). The emitted blackbody luminosity can be calculated making a best fit of temperature and hydrogen column density; it should be at least 10^{34} erg s^{-1}, far in excess of $L_{Br} + L_{cyc}$.

King and Lasota (1979a) sought to avoid these difficulties and proposed that the soft X-ray component is due to Bremsstrahlung by hot gas ($T = 3 \times 10^5$ K) surrounding the hard X-ray source. This could be consistent with the difference between the hydrogen column densities of the hard ($N_H \sim 10^{22}$ cm^{-2}, with large uncertainties) and soft ($N_H \sim 10^{20}$ cm^{-2}) components. However the UV observations, mentioned above, appear to favour the blackbody hypothesis (King and Lasota, 1980).

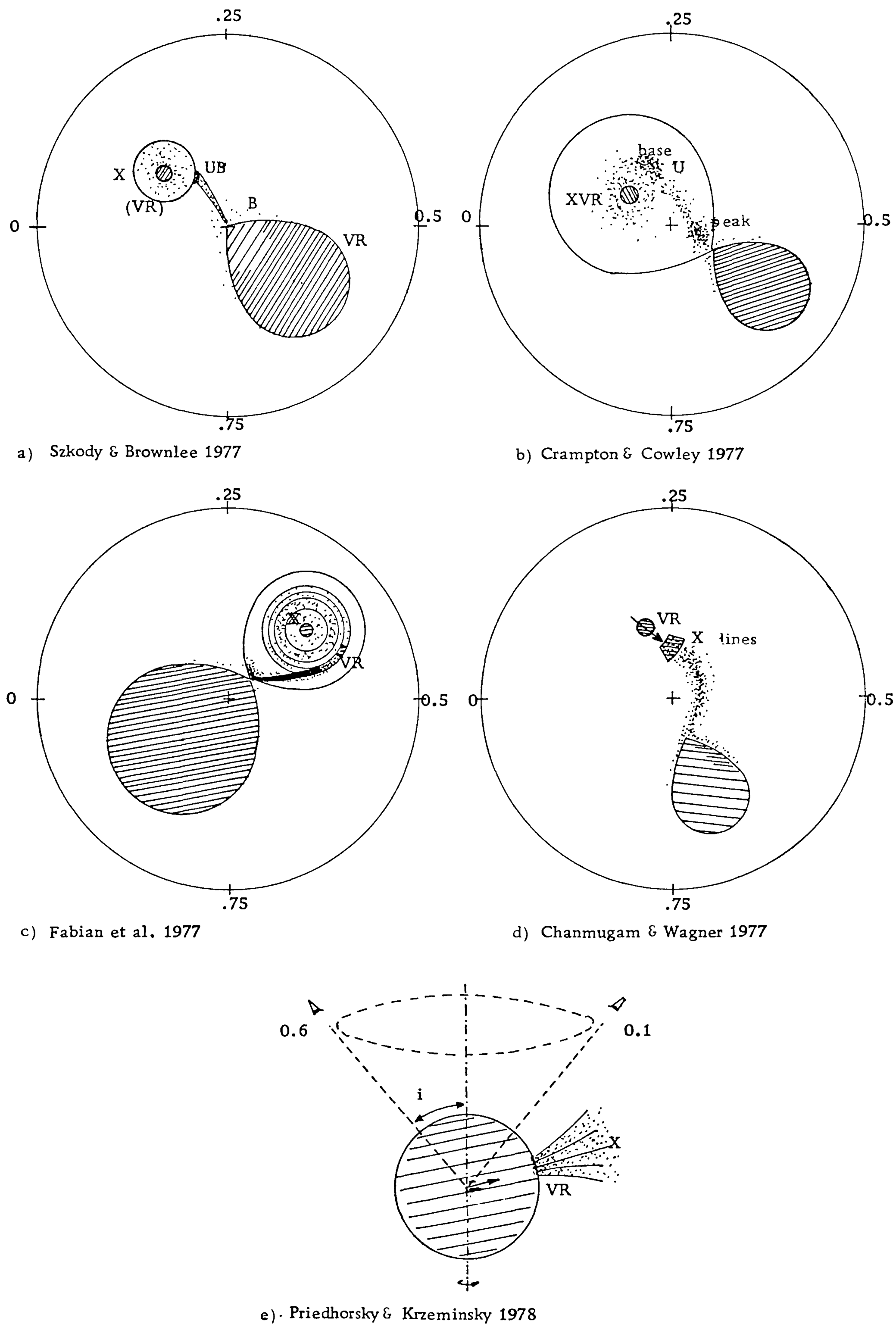

Fig. 10. Phase diagrams for some models of AM Her. All diagrams are properly aligned. Various sources of radiation (X-ray, UBVR band, lines) are indicated.

4.3. The geometry of AM Her

The unusual phasing of the velocity and light curves poses a serious problem in determining the geometry of the system. Phase diagrams, are collected in Figure 10.

The first schematic models (e.g. Szkody and Brownlee, 1977) described AM Her as similar to a cataclysmic variable: a red dwarf filling its Roche lobe and a white dwarf surrounded by an accretion disk. Szkody and Brownlee note however that no observational evidence of such a disk exists. The red dwarf was assumed as the main visible and red (VR) source (see Figure 10a). The light curve is explained as due to eclipse by the secondary and to X-ray heating effect: this is however criticized by Priedhorsky and Krzeminski (1978) because the angle subtended by the secondary is insufficient for both effects. In a further work Szekody (1978) attributes the VR flux to the proximity of the white dwarf.

In the model of Crampton and Cowley (1977) – see Figure 10b – a hot spot in the stream of matter is assumed as the source of the emission lines. This enables to explain the phasing between the velocity and light curves. A hot spot on an accretion disk plays also the role of the VR source in the model of Fabian *et al.* (1977) (see Figure 10c, see also King *et al.*, 1978). Priedhorsky *et al.* (1978b) note that the maxima of the light curve are similar while the minima are different: this favours models where minima are due obscuration rather than those in which maxima are due to a light excess contributed by a hot spot.

The calculation of the Alfvén radius (Section 4.1) given $R_A = 1\text{–}2 \times 10^{11}$ cm. Since R_A is greater (or at least comparable) to the separation of the system, an accretion disk cannot be formed (e.g. Chanmugam and Wagner, 1977). This difficulty is avoided by Fabian *et al.* (1977) with the hypothesis that the white dwarf is not co-rotating, but has a spin period ~ 1 min.

No observational evidence of a short period is available (Szkody, 1978; Stockman and Sargent, 1979). However there are theoretical arguments against spin-up (angular momentum balance between matter accreted and expelled from the system; Stockman *et al.* (1977), Chanmugam and Wagner (1978)) and in favour of synchronous rotation (magnetic locking; Stockman *et al.* (1977), Joss *et al.* (1979)). Moreover, no observational evidence of a short period is available (Szkody, 1978; Stockman and Sargent, 1979). Joss *et al.* (1979) suggest also that magnetostatic interaction in the synchronous state can produce oscillatory drifts in phase about exact synchronism with periods of 1–10 yr. These oscillations should appear as a periodic drift of the phase of polarization features with respect to those of photometric minima and perhaps as a long period modulation in the mass transfer rate, which could depend on the orientation of the dipole.

One is therefore led to consider a different scenario. According to the discussion of Section 4.1 matter is channelled in an accretion funnel or column onto magnetic poles. Both X-rays and VR (cyclotron) radiation originate in the column. The modulation is explained assuming a tilt angle between the magnetic and rotation axes.

Chanmugam and Wagner (1977, 1978) and Priedhorsky and Krzeminski (1978) consider single column models. Accretion occurs on an 'active' magnetic pole while the other pole is quiescent. The two models differ in the proposed modulation mechanisms. In Chanmugam and Wagner's model (see Figure 10d) the white dwarf is seen 'pole-on' at primary V minimum, which is due to self-absorption in the column. Half a period later X-ray eclipse and secondary V minimum occur: the eclipse is due to screening of the X-ray emitting region (close to the surface) by the white dwarf, and the V minimum is explained as occultation of the base of the column, while the higher parts can still be seen. According to Priedhorsky and Krzeminski (1978), the *primary* minimum is caused by screening of the VR source by the white dwarf (while the higher X-ray source is uneclipsed). Secondary and X-ray minima are explained as self-absorption in the column, which is viewed lengthwise at this phase (see Figure 10e).

The modulation of polarization can be interpreted, considering that circularly polarized radiation is emitted preferentially parallel to the magnetic field, and linearly polarized radiation perpendicular. An explanation of the sharpness of the linear polarization spike, based on Faraday effect and high harmonic cyclotron radiation, was proposed independently by Stockman (1977) and Chanmugam and Wagner (1978). Using Tapia's unpublished observations of linear polarization maxima (Tapia's spike at $\phi_M = 0.0$ and a shallower maximum at $\phi_M = 0.27$) the latter authors derive a relation between the inclination i and dipole tilt angle θ:

$$\cot \theta = -\cos \pi (\phi_{p\ \max\ 2} - \phi_{p\ \max\ 1}) \tan i = 0.66 \tan i . \tag{4.6}$$

Another argument in favour of this model is that, while hard X-rays can be emitted in the higher part of the column, soft X-rays (i.e. black-body) must be emitted at the surface of the white dwarf. In Priedhorsky and Krzeminski's model this implies a soft X-ray eclipse at primary V minimum, which is not observed.

On the other hand two observations favour Priedhorsky and Krzeminski's model. The first is the decrease of the width of primary minimum with increasing wavelength, discussed in the preceding section. The second is based on the line equivalent width variation (see Section 2.3). If the maximum intensity corresponds to the stream viewed lengthwise (which agrees with the radial velocity curves) and the stream is in line with the column, the occurrence of maximum equivalent width around the secondary minimum is in agreement with the model.

Also a two poles model has been proposed (Kruszewski, 1978, see also King and Lasota, 1979). The two poles have different magnetic field, accretion rate and critical cyclotron harmonic. At the strong (high magnetic field) pole, cyclotron dominates: this pole is the VR source, and no X-rays are emitted. The weak pole is the X-ray source, and also the far IR source (weaker B corresponds to longer cyclotron wavelength)which explains the similarity of the X-ray and 2.2 μm light curves. This fact could be easily explained also in a single pole model, where the far IR source lies higher in the column.

We note that a displacement of the dipole from the center of the white dwarf (i.e. different magnetic field intensity at the two poles) is not necessary to confine accretion or X-ray emission to one pole. If the secondary is contained within the

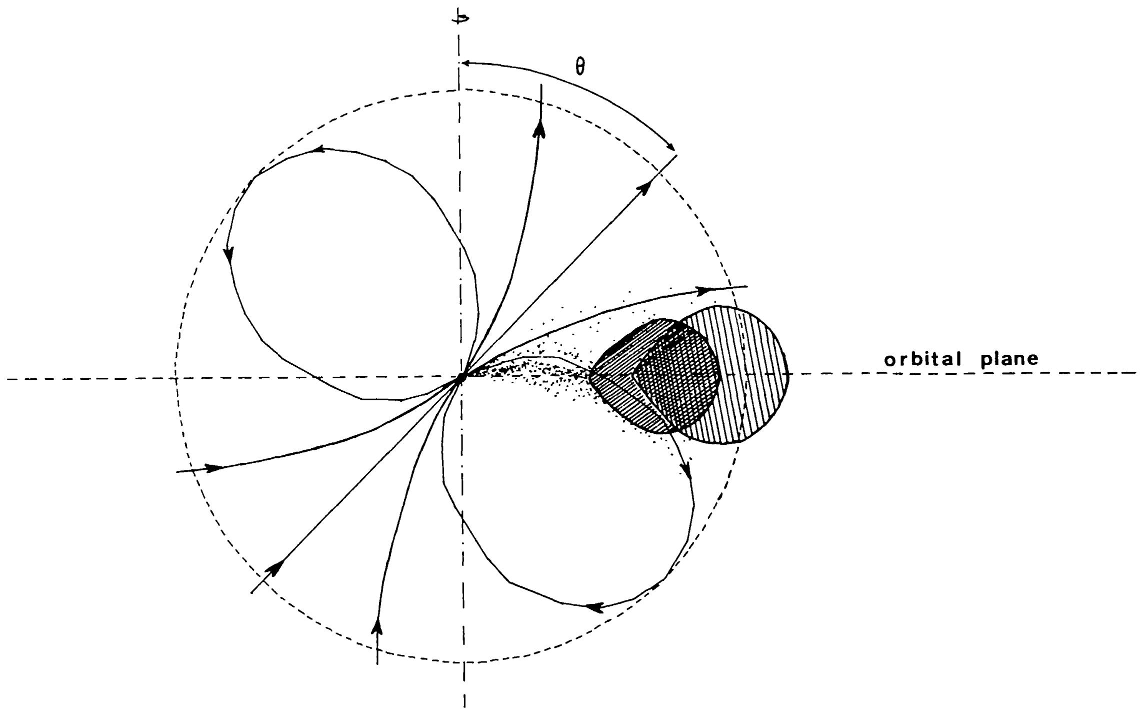

Fig. 11. The magnetosphere of AM Her. The Alfvén radius is 10^{11} cm. The size of the companion is consistent with a mass of $0.4M_\odot$ and a semiaxis 0.7×10^{11} cm (heavy dashed) or 0.9×10^{11} cm (light dashed).

magnetosphere of the white dwarf (as likely according to the value of the Alfvén radius, see Figure 11), it is contained also in a single accretion funnel, for tilt angles $90° > \theta > \theta_1$, with $\theta_1 = 55°–42°$ depending on the size of the secondary. Even for smaller θ most of the matter is accreted by the near pole, since mass loss from the secondary would be greater near the Lagrangian point.

5. Related Objects

AM Her may be considered as the prototype of a class of objects (sometimes called 'polars') (Krzeminski and Serkowski, 1977) with the following characteristics:

(a) close binary system with $P \ll 1$ d;
(b) one component is a highly magnetized white dwarf ($B \sim 10^8$ G);
(c) X-ray emission.

Besides AM Her, two objects with characteristics (a)–(c) are known. These are AN UMa and 2A 0311–227. The main parameters for these systems are reported in Table VIII, together with those of VV Pup, for which no X-ray emission has been detected by now. The magnetic field of VV Pup has been determined from observations of cyclotron absorption features (Visvanathan and Wickramasinghe, 1979). The source 2A0526–328 is identified with a 14 mag star, the spectrum of which resembles that of AM Her. Since it does not exhibit significant polarization ($p, q < 0.5\%$) it should be included in non magnetic cataclysmic variables (Charles *et al.*, 1979, and references therein).

TABLE VIII

Parameters of known AM Her type objects

Object	m_v		P	d	q_{max}	B	X-ray flux (erg cm^{-2} s^{-1})	
	HI	LO	(h)	(pc)	(%)	(G)	Soft	Hard
AM Her	11.9	15.0	3.1	75–130	9	2×10^8	5×10^{-10}	7.6×10^{-10}
AN UMa[1]	14	18.9	1.9	–	35	3×10^8	2.8×10^{-11}	–
2A0311[2]	13.8	15	1.35	–	6–9	–	2×10^{-11}	4.3×10^{-11}
VV Pup[3]	15	17.5	1.7	80–150	7–15	3×10^7	–	–

Sources: [1] General references: Kzreminski and Serkowski, 1977, and ref. therein; X-ray: Hearn and Marshall (1979).

[2] Identification: Williams *et al.* (1979), Griffiths *et al.* (1979); Soft X-ray and modulation: Hearn (1979) and Charles *et al.* (1979); Polarization: Tapia (1979); IR modulation: Ward (1979); Visible modulation: Bond *et al.* (1979).

[3] General references: Liebert *et al.* (1978); Magnetic field: Visvanathan and Wickramasinghe (1979); Stockman *et al.* (1979).

As indicated in Table II for at least three objects there is evidence of the existence of HI and LO states. In the optical band all objects have an emission line spectrum (Balmer, He I and He II lines) in the HI state. Lines disappear in the LO state in the case of VV Pup (Liebert *et al.*, 1978) and AN UMa (Liebert *et al.*, 1979).

The light curves exhibit substantial differences: for instance the X-ray minimum in AN UMa, unlike AM Her, occurs midway between optical linear polarization peaks (Hearn and Marshall, 1979).

VV Pup shows usually a very deep ($\Delta m = 2$) broad minimum, but sometimes a flat light curve, either in the HI or in the LO state. This is interpreted as due to the presence of two accreting poles of which one or both may be sometimes inactive (Visvanathan and Wicramasinghe, 1979; see also Liebert and Stockman, 1979). A different picture is offered by 2A0311–227 (Williams *et al.*, 1979; Bond *et al.*, 1979). These differences are however not such that the general structure of the models of AM Her cannot be applied to these sources (e.g. Liebert *et al.*, 1978; Liebert and Stockman, 1979).

The class of polars is obviously related to cataclysmic variables, some of which have been detected as X-ray sources: SS Cyg (Rappaport *et al.*, 1974; Fabbiano *et al.*, 1978, and references therein), U Gem (Mason *et al.*, 1978a; Swank *et al.*, 1978) EX Hya (Watson *et al.*, 1978); for X-ray survey of CV's see Watson *et al.* (1978) and Mason *et al.* (1978b). The main difference is the value of the magnetic field, which excludes for polars the formation of an accretion disk, and accounts for the X-ray modulation. For a discussion of the problem of X-ray production we refer in particular to Pringle (1977) and Pringle and Savonije (1979).

6. Concluding Remarks

AM Her is the first example of an accreting, X-ray emitting, magnetic white dwarf.

Its behaviour can be described by present theoretical models, but some difficulties and open questions still remain. Among the open problems of particular interest we shall list the following ones.

The evolutionary history of cataclysmic variables and AM Her type objects is very uncertain. In spite of its difficulty it would be a valuable task to develop an evolutionary scenario in analogy to those established for massive X-ray sources. In particular it would be of great interest to compare the expected density of polars (10^{-6}–3×10^{-7} pc^{-3}) with the observations. A systematic search of AM Her like objects is therefore also required (see e.g. Lamb, 1979; Stockman, 1979).

The theory of accreting white dwarfs should be improved. The major discrepancies between theory and observations are the lack of the cyclotron peak in the UV and the excess luminosity of the blackbody component.

The lack of cylotron emission in the UV is indicative of a magnetic field smaller than expected. For the only polar for which an accurate determination of B has been made (VV Pup) one has $B = 3 \times 10^7$ G (see Table II). Alternatively, Chanmugam (1979) suggests that if one takes into account the anisotropic cyclotron opacity and computes the angular distribution of radiation, the UV flux is 3–5 times less than predicted by the usual model.

With regard to the problem of the importance of the blackbody component (see Section 4.2) many explanations have been proposed. King and Lasota (1979b) have investigated the possibility of an accretion column where electron conduction dominates on radiative losses. Such a model gives $L_{bb} \gg L_{Br} + L_{cyc}$ as requested by observations. However detailed calculations by Imamura *et al.* (1979) in the non magnetic case show that the corrections due to electron conduction (greater soft X-ray luminosity, softer spectrum) does not exceed 25%. As mentioned in Section 4.1 a large blackbody luminosity can be obtained by steady nuclear burning. But nuclear burning occurs preferentially in outbursts (i.e. short active states separated by long quiescent periods) which is not the case of AM Her. A third possibility requires that a large fraction of the hard X-ray flux is backscattered to the stellar surface and absorbed. The issue is manifestly still unresolved and deserves further investigations.

Acknowledgements

We are deeply indebited to many colleagues for a critical reading of a preliminary version of the manuscript and for useful comments and suggestions. L. C. gratefully acknowledges a grant of the Foundation Blanceflor Boncompagni–Ludovisi Bildt, which made possible his stage at MSSL where this work was completed.

References

Aizu, K.: 1973, *Prog. Theor. Phys.* **49**, 776.
Angel, J. R. P.: 1978, *Ann. Rev. Astron. Astrophys.* **66**, 487.
Bailey, J. A., Mason, K. O., and Parkers, G. E.: 1977, *Monthly Notices Roy. Astron. Soc.* **180**, 9P.

Bailey, J. A. *et al.*: 1978, *Monthly Notices Roy. Astron. Soc.* **184**, 73P.

Berg, A. R. and Duthie, J. G.: 1977, *Astrophys. J.* **211**, 859.

Beyer, M.: 1950, *Untersuchungen des Lichtwechsels von 70 unperiodische Veraenderlichen*, Berlin, Akademie-Verlag.

Boley, F., Johns, M., and Maker, S.: 1979, *IAU Circ.* **3324**.

Bond, H. E. and Tifft, W. G.: 1974, *Publ. Astron. Soc. Pacific* **86**, 981.

Bond, H. E., Chanmugam, G., and Gianer, A. D.: 1979, *Astrophys. J.* **234**, L113.

Bunner, A. N.: 1978, *Astrophys. J.* **220**, 261.

Cameron, A. G. W. and Mock, M.: 1967, *Nature* **215**, 464.

Chanmugam, G.: 1979, *Proc. IAU Colloq.* **53** (to appear).

Chanmugam, G. and Wagner, R.: 1977, *Astrophys. J.* **213**, L13.

Chanmugam, G. and Wagner, R.: 1978, *Astrophys. J.* **222**, 641.

Chanmugam, G. and Wagner, R.: 1979, *Astrophys. J.* **232**, 895.

Charles, P. *et al.*: 1979, *Astrophys. J.* **231**, L131.

Coe, M. J., Engel, A. R., and Quenby, J. J.: 1978, *Nature* **272**, 37.

Coe, M. J. *et al.*: 1979, *Nature* **279**, 509.

Cooke, B. A. *et al.*: 1978, *Monthly Notices Roy. Astron. Soc.* **182**, 489.

Cowley, A. P. and Crampton, D.: 1977, *Astrophys. J.* **212**, L121.

Crampton, D. and Cowley, A. P.: 1977, *Publ. Astron. Soc. Pacific* **89**, 374.

De Gregoria, A. J.: 1974, *Astrophys. J.* **189**, 555.

Fabbiano, G. *et al.*: 1978, *Nature* **275**, 721.

Fabbiano, G. *et al.*: 1980, *Bull. Am. Astron. Soc.* **11**, 788.

Fabian, A. C., Pringle, J. E., and Rees, M. J.: 1976, *Monthly Notices Roy. Astron. Soc.* **175**, 43.

Fabian, A. C. *et al.*: 1977, *Monthly Notices Roy. Astron. Soc.* **179**, 9P.

Feigelson, E., Dexter, L., and Liller, W.: 1978, *Astrophys. J.* **222**, 263.

Giacconi, R. *et al.*: 1974, *Astrophys. J. Suppl.* **27**, 37.

Gilmozzi, E., Messi, R., and Natali, G.: 1978, *Astron. Astrophys.* **68**, L1.

Greenstein, G. L. *et al.*: 1977, *Astrophys. J.* **218**, L121.

Griffiths, R. E. *et al.*: 1979, *Astrophys. J.* **232**, L27.

Harris, D. E., Bahcall, N. A., and Strom, R. C.: 1977, *Astron. Astrophys.* **60**, 27.

Hayakawa, S. *et al.*: 1979, in W. A. Baity and L. E. Peterson (eds.), *IAU/COSPAR Symp. on X-ray Astronomy*, Innsbruck.

Hearn, D. R. and Marshall, F. J.: 1979, *Astrophys. J.* **232**, L21.

Hearn, D. R. and Richardson, J. A.: 1977, *Astrophys. J.* **213**, L115.

Hearn, D. R., Richardson, J. A., and Clark, G. W.: 1976, *Astrophys. J.* **210**, L23.

Hearn, D. R.: 1979, *IAU Circ.* **3326**.

Hoshi, A.: 1973, *Prog. Theor. Phys.* **49**, 1184.

Hudec R. and Meinunger, L.: 1976, *Inf. Bull. Var. Stars* **1184**.

Imamura, J. A. *et al.*: 1979, *Proc. IAU Colloq.* **53** (to appear).

Ingham, W. H., Brecher, K., and Wasserman, I.: 1976, *Astrophys. J.* **207**, 518.

Jameson, R. F. *et al.*: 1978, *Nature* **271**, 335.

Joss, P. C., Katz, J. I., and Rappaport, S. A.: 1979, *Astrophys. J.* **230**, 176.

Katz, J. J.: 1977, *Astrophys. J.* **215**, 265.

Kemp, J. C.: 1970, *Astrophys. J.* **162**, 169.

King, A. R. and Lasota, J. P.: 1979, *Monthly Notices Roy. Astron. Soc.* **188**, 163.

King, A. R. and Lasota, J. P.: 1980, *Monthly Notices Roy. Astron. Soc.* **191**, 721.

King, A. R., Raine, J. D., and Jameson, R. F.: 1978, *Astron. Astrophys.* **70**, 327.

Kylafis, N. D.: 1978, Ph.D. Thesis, University of Illinois (unpublished).

Kylafis, N. D. and Lamb, D. Q.: 1979, *Astrophys. J.* **228**, L105.

Kylafis, N. D. *et al.*: 1979, *Ann. N.Y. Acad. Sci.* (in press).

Kruszewski, A.: 1978, in A. N. Zytkow (ed.), *Nonstationary Evolution of Close Binaries*, PWN, Warsaw, p. 55.

Krzeminski, W. and Serkowski, K.: 1977, *Astrophys. J.* **216**, L45.

Lamb, F. K., Pethick, C., and Pines, D.: 1973, *Astrophys. J.* **184**, 271.

Lamb, D. Q. and Masters, A. R.: 1979, *Astrophys. J.* **234**, L117.

Liller, W.: 1976, *Sky Telesc.* **53**, 351.

Liebert, J. and Stockman, H. S.: 1979, *Astrophys. J.* **229**, 652.

Liebert, J. *et al.*: 1978, *Astrophys. J.* **225**, 201.

Liebert, J., Bond, H. E., and Grauer, A. D.: 1979, *IAU Circ.* **3335**.
Mason, K. O. *et al.*: 1978, *Astrophys. J.* **226**, L129.
Mason, K. O., Cordova, F., and Swank, J.: 1978, in W. A. Baity and L. Peterson (eds.), *IAU/COSPAR, Symp. on X-ray Astronomy*, Innsbruck.
Masters, A. R.: 1978, Ph.D. Thesis.
Masters, A. R. *et al.*: 1977, *Monthly Notices Roy. Astron. Soc.* **178**, 501.
Meinunger, L.: 1960, *Mitt. Ver. Sterne* **12**, 523.
Meinunger, L.: 1976, *Coord. Camp. Obs. X-ray Bin. Circ.*
Michalsky, J. J. *et al.*: 1977, *Astrophys. J.* **216**, L35.
Murray, S. S. and Ulmer, M. P.: 1976, *Astrophys. J.* **210**, 230.
Nagase, F.: 1979, private communication.
Olson, C. E.: 1977, *Astrophys. J.* **235**, 166.
Pravdo, S. H.: 1978, in W. A. Baity and L. Peterson (eds.), *IAU/COSPAR Symposium on X-ray Astronomy*, Innsbruck.
Prieshorsky, W. C.: 1977, *Astrophys. J.* **212**, L117.
Priedhorsky, W. C. and Krzeminski, W.: 1978, *Astrophys. J.* **219**, 597.
Priedhorsky, W. C. *et al.*: 1978a, *Astrophys. J.* **225**, 542.
Priedhorsky, W. C. *et al.*: 1978b, *Astrophys. J.* **226**, 397.
Pringle, J. E.: 1977, *Monthly Notices Roy. Astron. Soc.* **178**, 195.
Pringle, J. E. and Savonije, G. L.: 1979, *Monthly Notices Roy. Astron. Soc.* **187**, 777.
Rappaport, S. *et al.*: 1974, *Astrophys. J.* **188**, L47.
Raymond, J. C. *et al.*: 1979a, *Astrophys. J.* **230**, L95.
Raymond, J. C. *et al.*: 1979b, *IAU Symp.* **88**, (to appear).
Sazonov, V. B. and Chernomordik, V. V.: 1975, *Astrophys. Space Sci.* **32**, 355.
Staubert, R. *et al.*: 1978, *Astrophys. J.* **225**, L113.
Stockman, H. S.: 1977, *Astrophys. J.* **218**, L57.
Stockman, H. S.: 1979, *NASA Workshop on Observing Compact Objects.*
Stockman, H. S. and Sargent, T. A.: 1979, *Astrophys. J.* **227**, 197.
Stockman, H. S. *et al.*: 1977, *Astrophys. J.* **217**, 815.
Stockman, H. S., Liebert, J., and Bond, H. E.: 1979, *Proc. IAU Colloq.* **53** (to appear).
Swank, J. *et al.*: 1977, *Astrophys. J.* **216**, L71.
Swank, J. H. *et al.*: 1978, *Astrophys. J.* **226**, L133.
Szkody, P.: 1978, *Publ. Astron. Soc. Pacific* **90**, 61.
Szkody, P.: 1979, *Proc. IAU Colloq.* **51** (to appear).
Szkody, P. and Brownlee, D. E.: 1977, *Astrophys. J.* **212**, L113.
Tanzi, E. G. *et al.*: 1979, in A. J. Willis (ed.), *The First Year of IUE.*
Tanzi, E. G. *et al.*: 1980, *Astron. Astrophys.* **83**, 270.
Tapia, S.: 1977, *Astrophys. J.* **212**, L125.
Tapia, S.: 1979, *IAU Circ.* **3327**.
Tuohy, I. R. *et al.*: 1978, *Astrophys. J.* **226**, L17.
Tuohy, I. R., Mason, K. O., and Garmire, G. P.: 1980, in preparation.
Vojkhanskaja, M. P.: 1978, *IAU Circ.* **3224**.
Visvanathan, N. and Wickramasinghe, D. T.: 1979, *Nature* **281**, 47.
Ward, M. J. *et al.*: 1979, *IAU Circ.* **3335**.
Watson, M. G., Sherrington, M. R., and Jameson, R. F.: 1978, *Monthly Notices Roy. Astron. Soc.* **184**, 79P.
Weast, G. J. *et al.*: 1979, *Proc. IAU Colloq.* **53** (to appear).
Williams, G. *et al.*: 1979, *Nature* **281**, 48.
Wolf, M.: 1924, *Astron. Nachr.* **220**, 255.
Wright, E. L.: 1977, private communication to Hearn and Richardson (1977).
Young, P. and Schneider, D. P.: 1979, *Astrophys. J.* **230**, 502.